Polymer 55 (2014) 5623–5634

Contents lists available at ScienceDirect

Polymer

journal homepage: www.elsevier.com/locate/polymer

Synthesis, oxidation and crosslinking of tetramethyl bisphenol F (TMBPF)-based polymers for oxygen/nitrogen gas separations

Benjamin J. Sundell [a], Andrew T. Shaver [a], Qiang Liu [b], Ali Nebipasagil [a], Priya Pisipati [a], Sue J. Mecham [a, *], Judy S. Riffle [a], Benny D. Freeman [b], James E. McGrath [a]

[a] Macromolecules and Interfaces Institute, Virginia Tech, Blacksburg, VA 24061, USA
[b] Department of Chemical Engineering, Center for Energy and Environmental Resources, The University of Texas at Austin, Austin, TX 78758, USA

ARTICLE INFO

Article history:
Received 20 June 2014
Received in revised form
30 August 2014
Accepted 5 September 2014
Available online 21 September 2014

Keywords:
Poly(arylene ether)
UV crosslinking
Gas separation

ABSTRACT

Amorphous, high glass transition, crosslinkable poly(arylene ether)s for gas purification membranes have been synthesized. The polymers include a moiety capable of several oxidation reactions and UV crosslinking. Structural identification was confirmed by ^{1}H NMR and IR spectroscopy and molecular weights were determined by SEC. Two oxidation reactions of the polymers were identified, one by chemical treatment using Oxone and KBr and one by elevated thermal treatment in air. DSC and TGA were used for thermal characterization, and TGA, ^{1}H NMR and ATR-FTIR revealed the progress of the thermal oxidation reactions. Both polymers produced tough, ductile films and gas transport properties of the non-crosslinked linear polymers and crosslinked polymer are compared. The O_2 permeability of one exemplary non-crosslinked poly(arylene ether) was 2.8 Barrer, with an O_2/N_2 selectivity of 5.4. Following UV crosslinking, the O_2 permeability decreased to 1.8 Barrer, and the O_2/N_2 selectivity increased to 6.2.

1. Introduction

Polymeric membranes are important for the separation of gases in a variety of industrial applications [1]. Several excellent reviews have detailed industrial gas separations including the removal of carbon dioxide from natural gas [2], nitrogen enrichment from air [3], hydrogen recovery and a variety of smaller membrane markets [1,4]. These reviews also discuss some of the challenges associated with gas separation membranes such as achieving higher selectivity to provide higher purity products at high yield and making membranes more robust to harsh operating conditions and resistant to plasticization.

Transport of gases in dense polymeric membranes is based on the solution-diffusion model; the permeability of a gas across the membrane is the product of diffusion and solubility coefficients [3,5]. One measure of the ability of a membrane to separate a pair of gases is the ratio of the permeability coefficient of the more permeable gas to that of the less permeable gas, known as selectivity. The selectivity may be further separated into the product of solubility selectivity and diffusivity selectivity, the latter generally being the dominant factor controlling overall selectivity of glassy polymers [6]. Gas diffusion is very sensitive to the size of the diffusing gases and the availability of free volume within the polymer membrane [7,8]. A desirable gas separation membrane exhibits both high permeability and selectivity; however, an inherent trade-off relationship between these two properties has been identified. Membranes with high gas permeability typically have lower selectivity, and vice-versa. This observation led to the development of the concept of the upper-bound by Robeson, which is typically represented as a log–log plot of selectivity versus permeability [5]. The upper-bound plots were revised upwards once [9] based on the development of new classes of polymer membrane materials and have a mathematical and theoretical basis derived by Freeman [6]. Freeman, among others, noted that the most widely used approach to prepare materials with properties above the upper bound was to simultaneously increase polymer backbone stiffness and interrupt interchain packing to increase diffusivity.

Several families of glassy polymers have been investigated to explore the influence of polymer structure on gas transport properties. For example, one early effort studied the effect of tacticity on poly(methyl methacrylate) [10]. Polyimides typically have good gas separation properties and are of significant interest in the field because of their chemical robustness and low chain mobility

* Corresponding author. 145 ICTAS, Virginia Polytechnic Institute and State University, USA.
E-mail addresses: sjmecham@vt.edu, bsundell@vt.edu (S.J. Mecham).

http://dx.doi.org/10.1016/j.polymer.2014.09.010
0032-3861/

[11,12]. Another candidate for gas separation polymers is polysulfones due to their chemical stability and excellent mechanical properties, along with inherent rigidity due to in chain aromatic rings. The effect of variations in backbone chemical structure on permeability and selectivity of polysulfones has been studied [13,14]. For example, changes to the isopropylidene group, which influences bond rotation and intersegmental packing [15], the effect of symmetry of phenylene linkages, and methyl group placement [16] all have significant influence on gas separation properties of polysulfones. Several specialty polyimides have exceeded the upper bound by undergoing a chemical transformation to form carbon membranes at very high temperatures, such as that induced via pyrolysis between 550 and 800 °C [17]. Additionally, thermal rearrangement of *ortho*-positioned polyhydroxyimide precursors produce crosslinked polybenzoxazoles with much narrower pore size distributions than the precursor polyimides and, in some cases, gas separation properties beyond the upper bound [18].

One intriguing approach for improving the properties of gas separation membranes is to crosslink them, which is a well-known method to decrease chain mobility. In the late 1980s, Hayes demonstrated that UV crosslinked aromatic polyimides had a significantly higher selectivity than their linear analogs [19]. The effect of UV crosslinking on gas separation properties of the polyimides has been studied [20–23], and the effects of crosslinking have also been decoupled from thermal annealing [24,25]. These crosslinked membranes are especially effective in CO_2/CH_4 separations, because crosslinking greatly improves resistance to plasticization by CO_2 [26] or in some cases interrupts polymer crystallization [27].

In this paper, a poly(arylene ether sulfone) and poly(arylene ether ketone) have been synthesized from inexpensive reagents that contain moieties for UV crosslinking and an additional site for chemical oxidation. The materials considered in this study contain, in each repeat unit, a moiety derived from 4,4′-methylenebis(2,6-dimethylphenol), which has been used previously in polymers for forward osmosis [28] and as a self-cross-linked material for fuel cells [29]. This benzylic methylene group may be oxidized to a carbonyl by several routes and then UV crosslinked by benzylic hydrogen abstraction. This structure also provides the ability to UV crosslink a poly(arylene ether ketone) to increase backbone stiffness and interrupt chain packing by oxidizing the crosslinked polymeric backbone in the solid state. The synthesis and characterization of these polymers are described, and investigations of several oxidation routes are discussed. Initial film casting, UV crosslinking, and gas transport properties are also discussed.

2. Experimental

2.1. Materials

2,6-Dimethylphenol (2,6-xylenol, 99+%), 37% formaldehyde in H_2O (formalin), phosphorous pentoxide (P_2O_5), lithium bromide (LiBr) and potassium bromide (KBr) were purchased from Sigma–Aldrich. *N*-Methyl-2-pyrrolidone (NMP), methanol (MeOH) and sulfuric acid were purchased from Spectrum Chemical. Chloroform ($CHCl_3$), *N*,*N*-dimethylacetamide (DMAc) and acetonitrile (CH_3CN) were purchased from Fisher. DMAc used as a reaction solvent was dried with calcium hydride (CaH_2), distilled under reduced pressure and stored over 3 Å molecular sieves before use. Calcium hydride (90–95%) and potassium peroxymonosulfate (Oxone) were purchased from Alfa Aesar. Celite was purchased from EMD chemicals. 4,4′-Difluorobenzophenone (DFB) was purchased from TCI. 4,4′-Dichlorodiphenyl sulfone (DCDPS) was kindly provided by Solvay and recrystallized from toluene before use.

2.2. Synthesis of 4,4′-methylenebis(2,6-dimethylphenol)

The synthesis of 4,4′-methylenebis(2,6-dimethylphenol), tetramethyl bisphenol F, hereafter referred to as TMBPF, was adapted from a traditional synthesis of a phenol-formaldehyde resin [30]. Excess 2,6-xylenol (415.83 mmol, 50.80 g) was added to a 250-mL three-necked flask equipped with a condenser, mechanical stirrer, and addition funnel. The 2,6-xylenol was heated in a thermocouple regulated oil bath to 90 °C and stirred as it began to melt. Sulfuric acid (0.5 g) was added very slowly via the addition funnel, which changed the reaction solution to a dark pink color. The addition funnel was rinsed with DI water to ensure that all of the acid catalyst was transferred into the reaction flask. Formalin (37% by mass formaldehyde in H_2O, 15 mL) was added slowly via the addition funnel over the course of several hours; during this time, the reaction solution turned lighter in color and significantly more opaque. As more product continued to form, the reaction mixture transformed from a liquid to a solid. The crude product was removed from the flask and filtered using an aspirator and washed copiously with hot DI water. The crude product was dried at 70 °C in a convection oven and was recrystallized from MeOH to obtain a 90% yield.

2.3. Synthesis of bis-(2,6-xylenol)-F-DFB poly(arylene ether) ketone (TMBPF-DFB)

The TMBPF-DFB polymer was synthesized using a nucleophilic aromatic substitution procedure previously reported [31]. TMBPF (39.01 mmol, 10.0000 g), DFB (39.01 mmol, 8.5121 g) and DMAc (62 mL) were added to a 250-mL three necked flask. The reaction flask was equipped with a mechanical stirrer, nitrogen inlet, and Dean–Stark trap filled with toluene. A stirring, thermocouple regulated oil bath was heated to 155 °C. After a homogeneous solution was obtained and the oil bath was at 155 °C, K_2CO_3 (54.61 mmol, 7.5482 g) and toluene (31 mL) were added, which immediately turned the light yellow solution a deep violet color. The reaction was stirred at 155 °C for 3 h to azeotropically remove any water, and then the bath was heated to 175 °C. Toluene and water were drained from the Dean Stark trap, and the reaction was maintained at this final temperature overnight. After 16 h, the viscous solution was diluted with additional DMAc (62 mL) and filtered through celite using an aspirator. The polymer solution was precipitated into rapidly stirring DI water to produce a fibrous white solid, filtered using an aspirator, and then boiled several times in DI water to remove any residual salt by-product. The solid polymer was finally dried at 150 °C in *vacuo*.

2.4. Synthesis of bis-(2,6-xylenol)-F-DCDPS poly(arylene ether) sulfone (TMBPF-DCDPS)

The TMBPF-DCDPS polymer was synthesized in the same manner as the TMBPF-DBF polymer, except DCDPS (39.01 mmol, 11.2023 g) was used instead of DFB, and more DMAc (71 mL) was used to obtain the same monomer concentration due to higher total monomer mass.

2.5. Oxidation of TMBPF-DCDPS polymer with Oxone/KBr

Oxidation of the TMBPF-DCDPS polymer was adapted from a literature procedure for the oxidation of small molecules with benzylic methylene linkages [32]. TMBPF-DCDPS polymer (1.0 g) was added to CH_3CN (26 mL) and DI water (2 mL) in a 100-mL round bottom flask. Oxone (4.675 mmol, 0.712 g) and KBr (1.063 mmol, 0.126 g) were added to the flask. The flask, under air, was sealed with septa and stirred in a thermocouple regulated water bath at 45 °C. After several hours, the temperature was raised

to 60 °C, and the reaction was stirred overnight. The heterogeneous reaction was poured directly into stirring DI water (250 mL), stirred for several hours, filtered on an aspirator, and dried overnight at 70 °C in a convection oven.

2.6. Thermal oxidation of TMBPF polymers

The TMBPF polymers were thermally treated in air in a Lindberg/Blue M 1200 °C box furnace. Once the oven reached the specified temperature, the polymer inside of an open scintillation vial was placed into the oven. After a designated time, the vial was removed and sealed for analysis.

2.7. Structural characterization

Proton nuclear magnetic resonance (^{1}H NMR) spectroscopy was performed on a Varian Inova spectrometer operating at 400 MHz. All spectra were obtained from 15% (w/v) 1 mL solutions in deuterated chloroform ($CDCl_3$). Fourier Transform Infrared Spectroscopy with attenuated total reflectance (FTIR-ATR) was applied to the polymers to observe the conversion of the methylene bridge to the carbonyl group as a result of oxidation. The FTIR-ATR spectra were recorded on an FTIR spectrometer (Varian 670 FTIR) equipped with an ATR attachment with a diamond crystal. The spectral resolution was 4 cm^{-1}, and 32 background scans were performed. A small amount of polymer was placed on the diamond crystal, and the FTIR spectrum was measured with 32 scans. The spectra were baseline corrected and normalized based on the initial C═O group stretch at ca. 1525 cm^{-1}. All measurements were performed at ambient temperature. Intrinsic viscosities (IV) and molecular weights of the polymers were obtained by size exclusion chromatography (SEC). The SEC system consisted of an isocratic pump (Agilent 1260 infinity, Agilent Technologies, Santa Clara, CA) with an online degasser (Agilent 1260, Agilent Technologies, Santa Clara, CA), autosampler and column oven used for mobile phase delivery and sample injection, and three Agilent PLgel 10 μm Mixed B-LS columns 300 × 7.5 mm connected in series with a guard column as the stationary phase. A system of multiple detectors connected in series was used for the analysis. A multi-angle laser light scattering (MALS) detector (DAWN-HELEOS II, Wyatt Technology Corporation, Goleta, CA), operating at a wavelength of 658 nm, a viscometer detector (Viscostar, Wyatt Technology Corporation, Goleta, CA), and a refractive index detector operating at a wavelength of 658 nm (Optilab T-rEX, Wyatt Technology Corporation, Goleta, CA) provided online results. The system was corrected for interdetector delay, band broadening, and the MALS signals were normalized using a 21,720 g/mol polystyrene standard obtained from Agilent Technologies or Varian. Data acquisition and analysis was conducted using Astra 6 software (Wyatt Technology Corporation, Goleta, CA). The mobile phase was NMP, which was vacuum distilled over P_2O_5 before use. The salt, 0.05 M dried LiBr, was added and dissolved in the NMP before the solvent was degassed and filtered. The sample solutions were prepared in a concentration range of 2~3 mg/mL and were filtered to remove any dust or insoluble particles using 0.22 μm PTFE filters. Molecular weight values were measured using light scattering, and the intrinsic viscosity values were measured online. Specific refractive index increment (dn/dc) values were calculated for each backbone type based on 100% mass recovery using the Astra 6 software.

2.8. Thermogravimetric analysis (TGA)

The thermal stability and oxidation of the polymers were investigated using a TA Instruments TGA Q5000. The polymers were first heated under a nitrogen atmosphere at a rate of 10 °C min^{-1} to 600 °C to test the thermal stability in an inert atmosphere. The thermal oxidation reaction and consequent weight gain were performed in air by heating at 10 °C min^{-1} to 220 °C, then 1 °C min^{-1} to 450 °C, and finally 10 °C min^{-1} to 700 °C.

2.9. Differential scanning calorimetry (DSC)

The glass transition temperatures (T_g) of the polymers were investigated with a TA Instruments DSC Q200. The polymers were heated under nitrogen at a rate of 10 °C min^{-1} to 350 °C, cooled to 50 °C, and heated again at a rate of 10 °C min^{-1} to 350 °C. The DSC thermograms shown are the second scan.

2.10. Film preparation

To prepare films, 0.8 g of polymer was added to 20 mL of chloroform ($CHCl_3$) in a scintillation vial, and the mixture was stirred until a homogeneous, transparent solution was obtained. The solution was syringe filtered through a 1.0 μm filter into a new vial. The vial was sonicated 3 times for 60 min each to remove dissolved gases. The solution was cast on a 10 × 15 cm clean, dry glass plate on a level casting surface and then dried in air at ambient conditions overnight. The following day the air dried film was removed, the edges were trimmed, and the film was dried at 120 °C under vacuum before gas transport experiments. TGA thermograms showed that these drying conditions were suitable for the complete removal of solvent.

2.11. UV crosslinking

Crosslinking was performed by irradiating polymer films in air under a 100 W high intensity, long-wave UV lamp equipped with a 365-nm light filter (Blak-Ray B-100, UVP). The film was placed about 3.5 cm from the UV lamp and irradiated for one hour on each side. At this distance, the UV intensity was measured to be 19.7 mW cm^{-2}.

2.12. Gel fractions

Crosslinked films were dried at 120 °C under vacuum overnight. Then 0.1–0.2 g of the crosslinked film was placed in a 20 mL scintillation vial filled with $CHCl_3$ and stirred overnight. The remaining solid was filtered, transferred to a pre-weighed vial, and dried at 120 °C under vacuum overnight to the final weight. Gel Fractions were calculated by equation (1) to determine the degree of crosslinking.

$$\text{Gel Fraction } (\%) = \frac{W_{\text{final}}}{W_{\text{initial}}} \times 100 \quad (1)$$

2.13. Density measurements

Density was measured using a Mettler Toledo balance equipped with a density measurement kit. Ethanol was chosen as the reference liquid because the samples tested showed low ethanol uptake over the time scale of the density measurement.

2.14. Gas permeation measurements

Gas permeation properties were measured using a constant-volume/variable-pressure method [33]. The upstream portion of the system was constructed from commercially available Swagelok parts using Swagelok tube fittings. Welded joints and VCR connections were used in the downstream portion to minimize leaks. The membrane was housed in a stainless steel Millipore filter

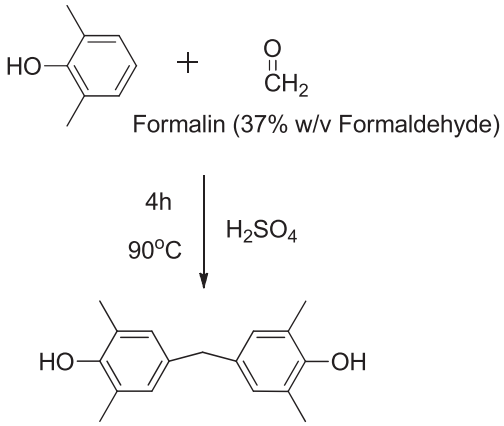

Fig. 1. Synthesis of TMBPF via electrophilic aromatic substitution.

holder (Millipore, Billerica, MA, USA) with an included support. A Honeywell Super TJE 1500 psi (10.3 MPa) transducer (Honeywell Sensotec, Columbus, Ohio, USA) was used to track upstream pressure, and a MKS Baratron 626 transducer (MKS, Andover, MA, USA) was used to measure downstream pressure. The permeabilities of N_2 and O_2 were measured at 35 °C at 10 atm feed pressure.

3. Results and discussion

3.1. Synthesis of tetramethyl bisphenol F monomer (TMBPF)

An appealing feature of these polymers is the low cost of starting materials. The TMBPF monomer is commercially available, or may be easily synthesized from inexpensive 2,6-xylenol and formalin via electrophilic aromatic substitution as shown in Fig. 1.

TMBPF is the key monomer in these polymers, because the benzylic methyl groups are necessary for UV crosslinking and the benzylic methylene group may undergo an oxidative chemical transformation [32]. A slight excess of 2,6-xylenol was used to drive the reaction to completion [34]. The reaction occurs very rapidly at the conditions used; however a temperature of 90 °C was necessary to ensure that the 2,6-xylenol was melted and that homogeneous stirring could occur. Upon formalin addition, the reaction shifted from a liquid to solid phase in addition to exhibiting a color change, which indicates the formation of product as TMBPF has a significantly higher melting point than 90 °C and is insoluble in water. Isolation of the monomer product was also very efficient. Washing with near boiling water is effective at removing residual acid and residual starting material. Upon drying, any residual 2,6-xylenol impurity in the crude product was assessed qualitatively by the presence of an orange/pink color, which is completely removed when recrystallized from methanol to yield white crystals.

3.2. Characterization of TMBPF monomer

The ^{1}H NMR spectrum of TMBPF is shown in Fig. 2. All of the peaks integrate quantitatively with regard to the molecular structure. The ^{1}H NMR also showed no organic side products or contaminants, including starting material. The melting point of the recrystallized product was measured via melting point apparatus and found to be in good agreement with reported values (177 °C) [35].

3.3. Synthesis and NMR of TMBPF polymers

Poly(arylene ether)s are potentially important candidates for gas separation materials, and poly(arylene ether sulfone)s in particular have already found wide application in the field [1,36]. The success of poly(arylene ether)s as gas separation membranes is in part due to their mechanical robustness and high chemical stability [37,38].

The TMBPF containing poly(arylene ether ketone) (TMBPF-DFB) and poly(arylene ether sulfone) (TMBPF-DCDPS) in this study were synthesized by nucleophilic aromatic substitution with a weak base [31,39]. The syntheses of the poly(arylene ether sulfone) and poly(arylene ether ketone) are shown in Figs. 3 and 4 respectively. Upon addition of toluene and K_2CO_3, both reaction solutions turned a deep violet color immediately, which persisted throughout the course of the reaction. In both reactions, toluene was used as an azeotropic solvent to remove water formed by K_2CO_3 reaction and subsequent decomposition. Water could potentially react with the activated dihalide monomer at higher temperatures and upset the reaction stoichiometry, leading to low molecular weight polymers. It was important to use a heat gun to dry the joints on the three-necked flask during the azeotropic reflux, where water may

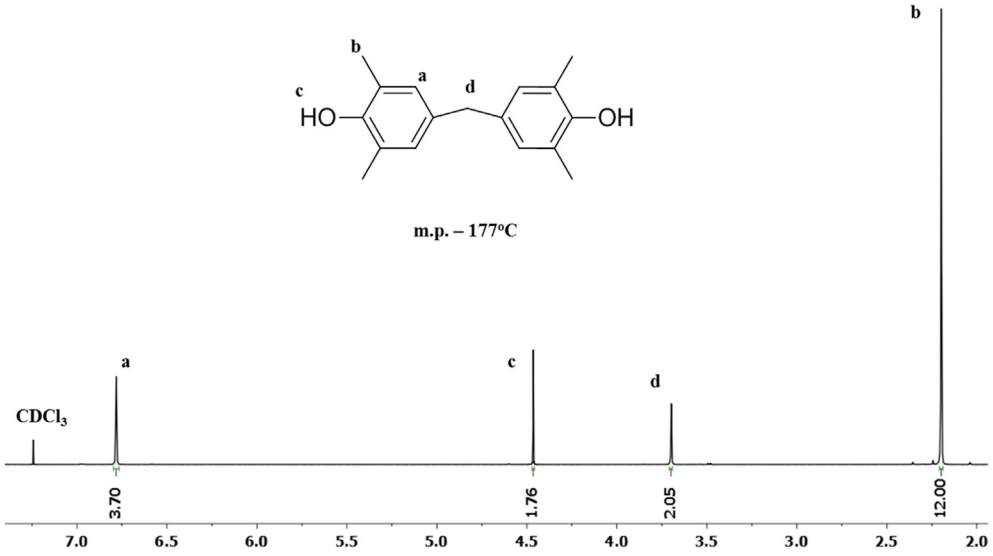

Fig. 2. ^{1}H NMR spectrum of TMBPF monomer.

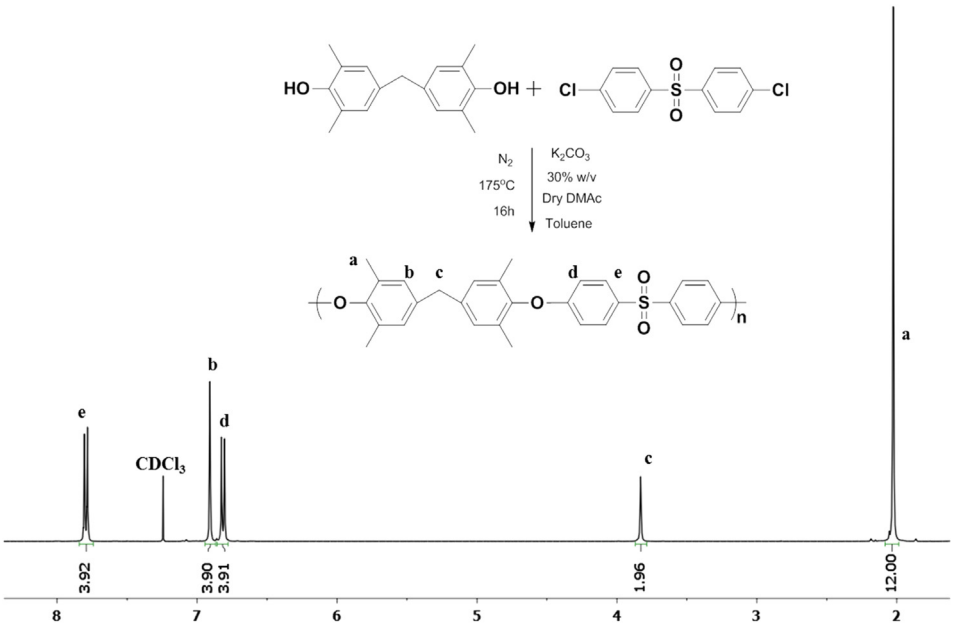

Fig. 3. Synthesis and ^{1}H NMR spectrum of TMBPF-DCDPS polymer.

become trapped. After the water was removed from the reaction, toluene was drained, and the flask was brought to the final reaction temperature. Difluorobenzophenone is a more reactive than dichlorodiphenyl sulfone, because the carbon fluorine bond is more polarized than the carbon chlorine bond, and therefore, more efficiently stabilizes the Meisenheimer complex intermediate [40]. Thus, the final temperature of the poly(arylene ether ketone) reaction was 20 °C lower than that of the poly(arylene ether sulfone) reaction. Both reactions exhibited high viscosity after 16 h and were stopped at this time.

After polymer isolation and drying, the TMBPF polymers were characterized by a variety of spectral and thermal methods. ^{1}H NMR was performed to ensure polymer purity, structural identification and removal of solvent. Figs. 3 and 4 demonstrate that all of these objectives were achieved, as the integrations corresponded to the expected structures and no impurities or endgroups were observed in the spectra, an indication of high molecular weight.

3.4. SEC of TMBPF polymers

The polymers were sufficiently high in molecular weight to form transparent, ductile films. SEC of the polymers quantitatively substantiated high molecular weight, and these results are shown in Fig. 5 and Table 1. The polymers have a monomodal Gaussian

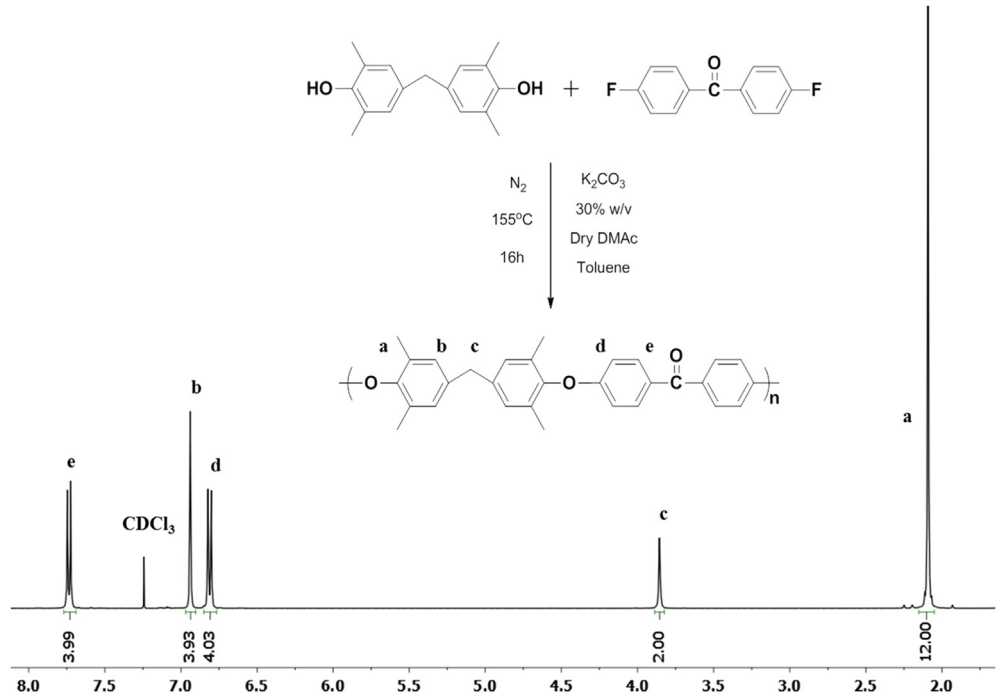

Fig. 4. Synthesis and ^{1}H NMR spectrum of TMBPF-DFB polymer.

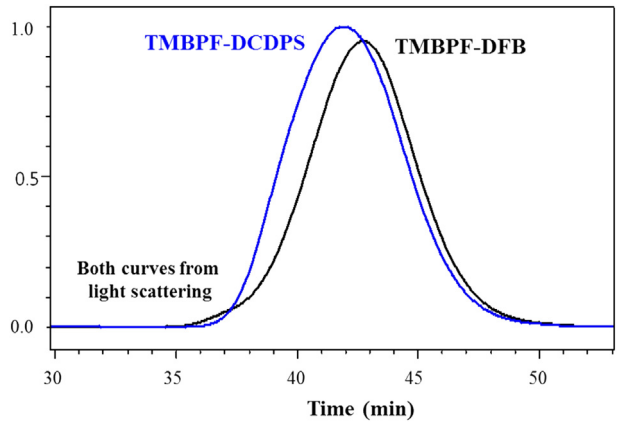

Fig. 5. SEC of TMBPF containing polymers.

Table 1
SEC of TMBPF containing polymers.

Sample	Mn (kDa)	Mw (kDa)	PDI	[η] (dL/g)	dn/dc (mL/g)
TMBPF-DCDPS	66.2	127.5	1.9	0.61	0.14
TMBPF-DFB	51.7	92.7	1.8	0.54	0.15

distribution and polydispersity index (PDI) that one would expect from a step growth polymerization. The PDI should theoretically be 2. However, some lower molecular weight material is likely lost during polymer isolation, thereby decreasing the observed PDI.

3.5. Oxidation of TMBPF-DCDPS polymer with Oxone/KBr

To UV crosslink these polymers requires the presence of aromatic carbonyl groups in the backbone and benzylic methyl groups [41]. The methylene bridge of the TMBPF group in the backbone of the polymer can be converted to a carbonyl via oxidation [42]. The oxidation of the TMBPF containing poly(arylene ether sulfone) was initially attempted using potassium peroxymonosulfate (Oxone®) and KBr in a procedure adapted from the oxidation of small molecules containing benzylic methylene linkages [32]. The poly(arylene ether sulfone) was initially tested for this oxidation route because the un-oxidized form does not contain carbonyl linkages, so the success of this reaction may be followed by tracking the growth of this peak by FTIR spectroscopy.

The small molecule procedure called for the addition of Oxone and KBr by molar equivalencies of 2.2 and 0.5 respectively. Because each repeat unit contains one benzylic methylene group capable of oxidation, the molecular weight of the repeat unit was used as the molar mass to determine 1 equivalent for stoichiometric considerations.

Addition of TMBPF-DCDPS polymer to aqueous acetonitrile turned the liquid a light amber color, and addition of Oxone and KBr produced a slight red tint that quickly disappeared upon stirring. It was apparent that the polymer was mostly insoluble in the solvent mixture, and gradually heating to 45 °C or 60 °C did not noticeably improve the solubility. The solvent system of aqueous acetonitrile was important for the success of oxidation in the small molecule reactions [32]. Water is the source of oxygen in the oxidized product, and changing the solvent to DMSO or DMF produced very low yields. One reaction for oxidizing TMBPF-DCDPS was performed in chloroform, a good solvent for this polymer, but this led to similar levels of conversion with side reactions including crosslinking.

Spectral verification of the oxidation reaction was done using ^{1}H NMR and FTIR-ATR spectroscopy. The ^{1}H NMR spectra of TMBPF-DCDPS and its partially oxidized analog are shown in Fig. 6. Most notably, the benzylic methylene peak *c* decreased to about 80% of its initial value, indicating near 20% conversion to the oxidized product. The peaks nearest to the benzylic methylene moiety, *a* and

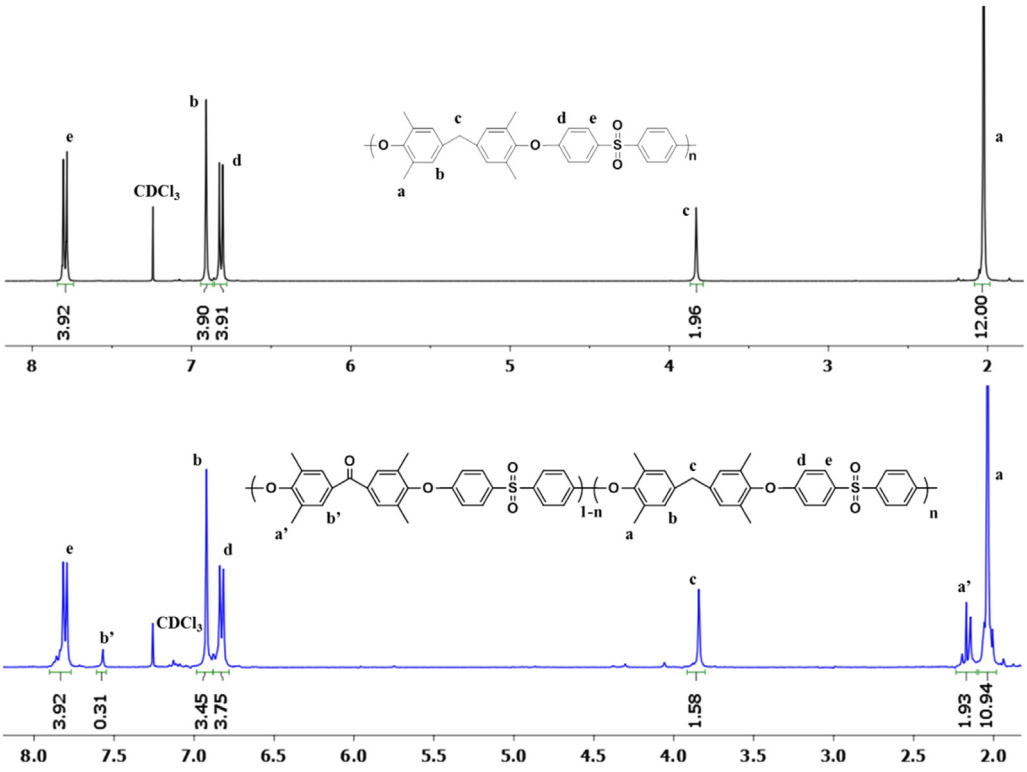

Fig. 6. ^{1}H NMR of TMBPF-DCDPS before and after oxidation with Oxone/KBr.

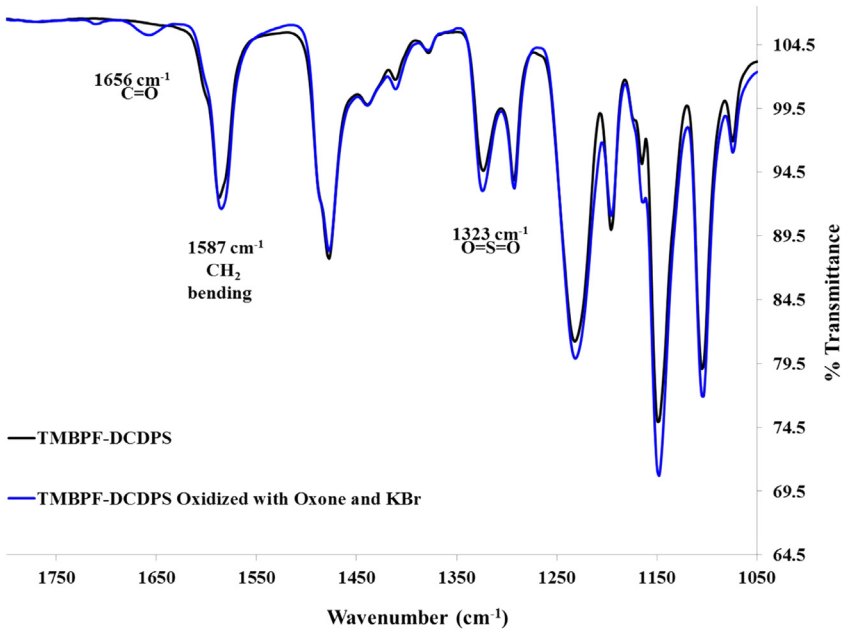

Fig. 7. IR of TMBPF-DCDPS before and after oxidation with Oxone/KBr.

b, also decreased and new peaks, *a′* and *b′* appeared downfield relative to the initial control peaks. This downfield shift is consistent with the electron withdrawing nature of the new carbonyl linkage compared to the original methylene group. Peaks *d* and *e* are less affected by this chemical transformation because of their distance from the methylene or carbonyl group, but a broadening of these peaks was still observed. FTIR-ATR spectra of the TMBPF-DCDPS polymer and its partially oxidized analog are presented in Fig. 7. Several signature peaks of the control polymer structure are highlighted, including the sulfone linkage and the benzylic methylene linkage. Most importantly, the partially oxidized polymer had a signature peak at 1656 cm^{-1}, indicating the appearance of a carbonyl group not observed in the control polymer.

3.6. UV crosslinking of oxidized TMBPF-DCDPS polymer

One important test on the partially oxidized TMBPF-DCDPS polymer was the ability of the polymer to UV self-crosslink. The UV crosslinking mechanism of interest was benzylic hydrogen abstraction by a benzophenone moiety, which generated two radicals that led to a crosslinked site upon recombination [43]. The TMBPF-DCDPS control polymer lacked the benzophenone moiety and was incapable of UV crosslinking. Two films were prepared to test the self-crosslinking reaction, one of the TMBPF-DCDPS control and one of the partially oxidized system. Both films were cast from chloroform, dried, and then exposed to UV light. After irradiation, both films were weighed and extracted with chloroform. The TMBPF-DCDPS film quickly dissolved, indicating 0% gel fraction and no crosslinking. However, the partially oxidized TMBPF-DCDPS film was largely undissolved after one day and had a gel fraction of 80%, demonstrating a high level of network formation.

3.7. TGA of TMBPF polymers under N_2

In addition to chemical and mechanical stability, high thermal stability is also desired for gas separation membranes. Some hydrogen separations are performed near 100 °C today, and there is discussion of performing separations at even higher temperatures, such as those involved in production of synthesis gas, which potentially require membrane stability above 300 °C [1], and pre-combustion carbon capture, which might need membranes that are stable at up to 150 °C or higher [44]. The thermal stability of the TMBPF polymers was initially tested under pure nitrogen, as shown in Fig. 8. Both polymers had very high thermal stabilities, showing no weight loss until 400 °C and a 10% weight loss above 450 °C.

3.8. TGA of TMBPF polymers in air

TGA of the TMBPF polymers was also performed in air, and the results are presented in Fig. 9. The polymers both showed a very interesting phenomenon, weight gain in the region of 250–325 °C. Initially, these polymers were only investigated for their ability to chemically oxidize, but it became apparent that the benzylic methylene linkage could also thermally oxidize at elevated

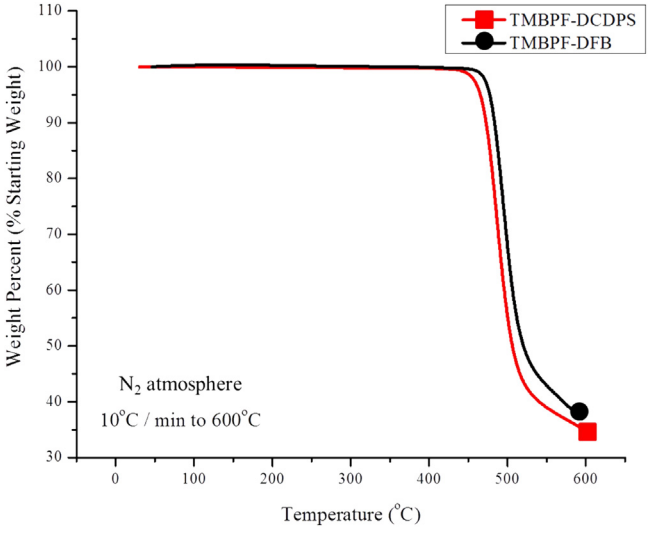

Fig. 8. TGA of TMBPF containing polymers in N_2.

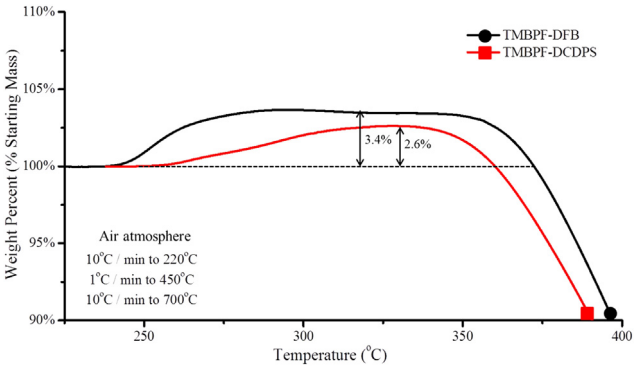

Fig. 9. TGA of TMBPF containing polymers in air.

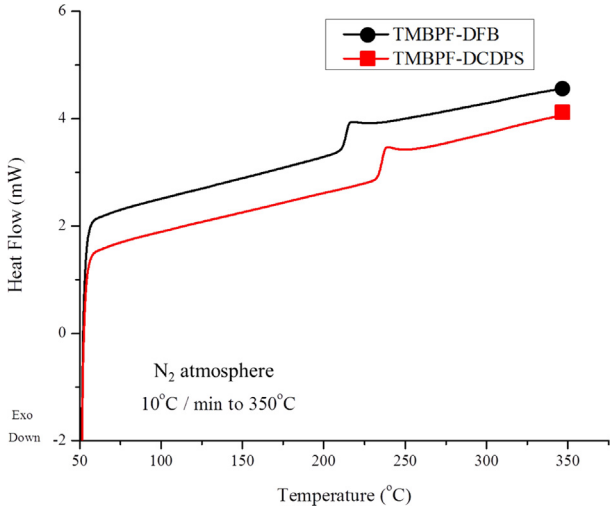

Fig. 10. DSC of TMBPF containing polymers in N_2.

temperatures in the presence of oxygen. The molecular mass difference between non-oxidized and oxidized polymer was calculated for both TMBPF containing poly(arylene ether ketone) and poly(arylene ether sulfone). The theoretical weight gain required to oxidize each methylene group to a carbonyl in the TMBPF-DFB polymer was 3.2%, and it was 3.0% for the TMBPF-DCDPS polymer. The theoretical weight percent increase was higher for the ketone system because of its lower molecular weight repeat unit. The actual weight gains shown in Fig. 9 were approximately 90% of the theoretically possible weight gains, suggesting a high level of oxidation. The temperature ramp above 220 °C was done at 1 °C/min, because incomplete oxidation was observed at higher heating rates (i.e., 10 °C/min). The rates of thermal oxidation at various fixed temperatures will be detailed in a subsequent publication.

3.9. Thermal properties of TMBPF polymers under N_2

DSC was performed to identify the glass transition temperatures (T_g's) of the TMBPF polymers. The samples were heated to 350 °C to erase their thermal history, cooled, and then heated again to 350 °C to produce the thermograms in Fig. 10. DSC was performed under an inert atmosphere to eliminate the possibility of thermal oxidation. Distinct endothermic transitions indicative of the T_g were found at 213 °C for TMBPF-DFB and 235 °C TMBPF-DCDPS. The T_g's were in the range expected for poly(arylene ethers); notably, the T_g of TMBPF-DCDPS was in excellent agreement with a prior literature study investigating the effect of polysulfone backbone structure on T_g [45]. The poly(arylene ether sulfone) has a T_g more than 20 °C higher than that of the poly(arylene ether ketone), likely due to the increased restrictions to rotation about the sulfone linkage relative to the carbonyl linkage. Results indicated that thermal oxidation in air began nearly 20 °C above the T_g of the polymers, as shown in Fig. 9 by weight gain. These results seem to suggest that extensive chain motion is needed for the oxidation process.

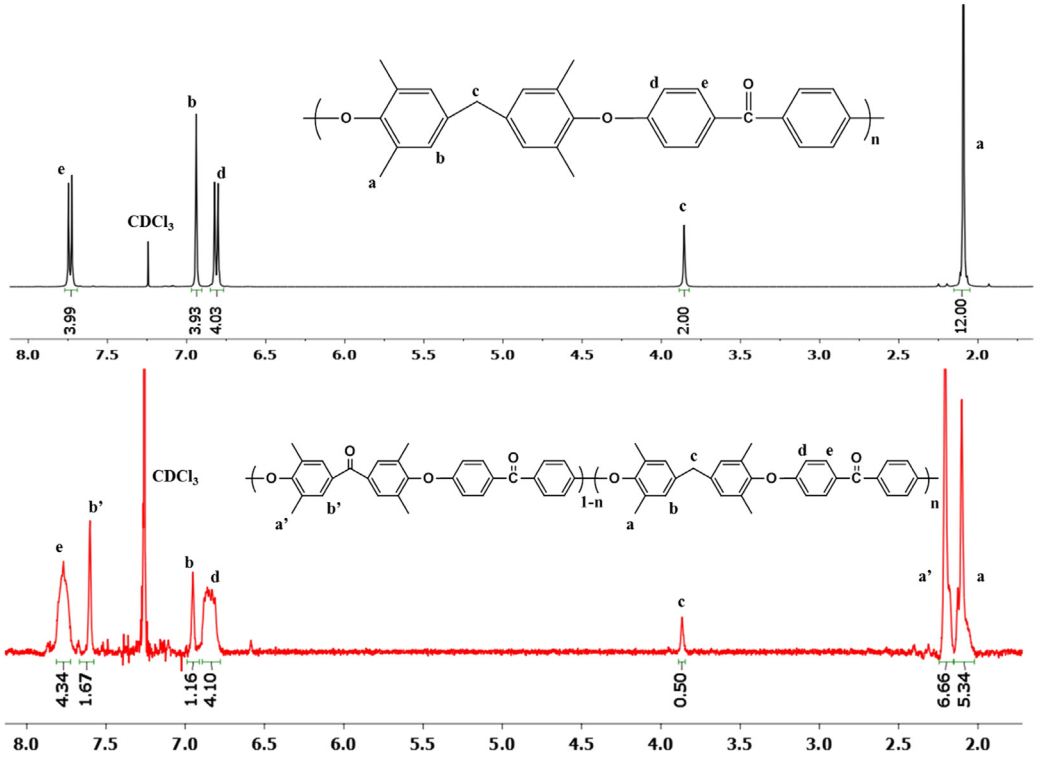

Fig. 11. ^{1}H NMR of thermally oxidized TMBPF-DFB.

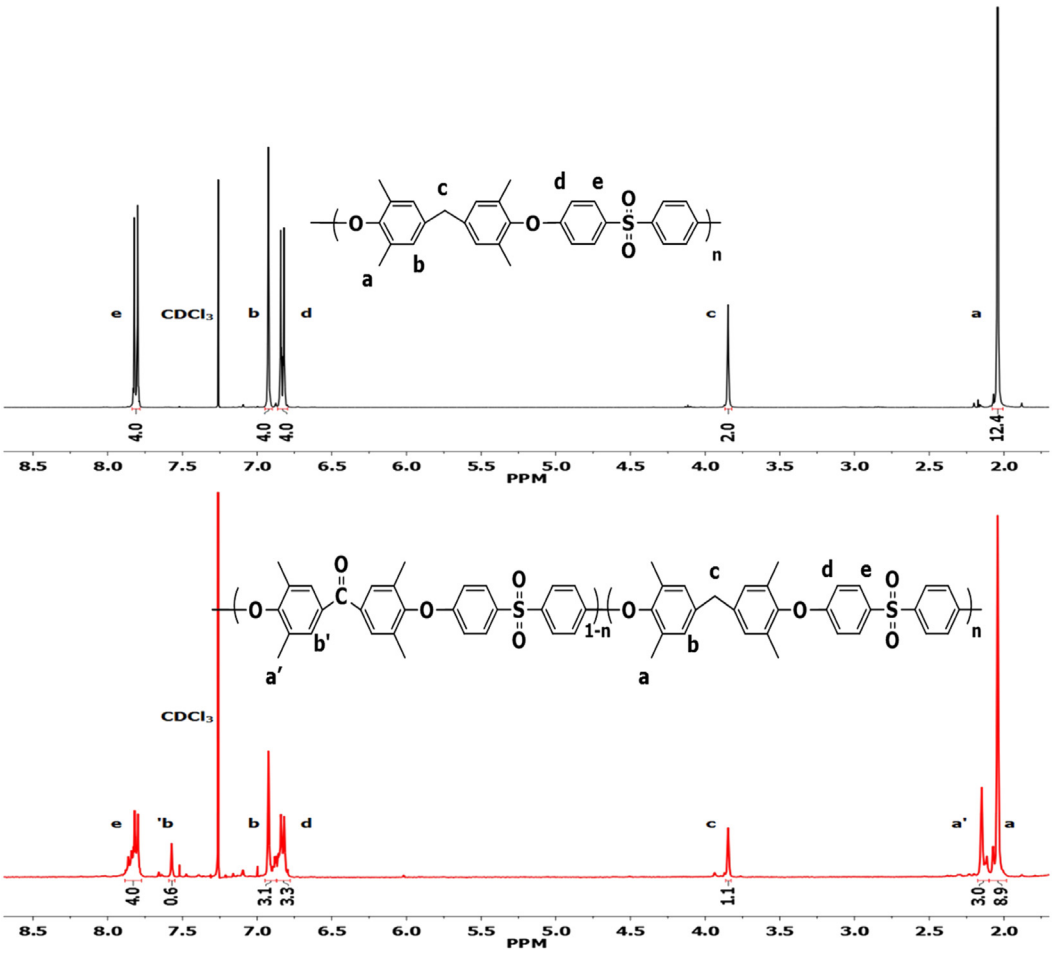

Fig. 12. ^{1}H NMR of thermally oxidized TMBPF-DCDPS.

3.10. NMR of thermally oxidized TMBPF-DFB polymer

To further test the thermal oxidation reactions, the TMBPF-DFB polymer was heated in air to 260 °C, well above T_g, and held for 10 min. The TMBPF-DCDPS polymer was heated to 280 °C in air, well above T_g, and held for 120 min. The TMBPF-DCDPS polymer was heated at a higher temperature and for a longer period of time to account for the slower oxidation rates observed via TGA. During these times, the polymers changed from white to a light yellow color. The ^{1}H NMR spectrum of the soluble fraction of the thermally oxidized TMBPF-DFB is shown in Fig. 11, and the spectrum for oxidized TMBPF-DCDPS is shown in Fig. 12.

Similar to the results obtained via partial Oxone/KBr oxidation, the thermal oxidation reactions were analyzed by ^{1}H NMR spectroscopy. The spectra show that the TMBPF-DFB polymer was oxidized to 75% conversion, and the TMBPF-DCDPS polymer was oxidized to 45% conversion, based on integration of the benzylic methylene peak (i.e., peak c in Figs. 11 and 12) before and after thermal oxidation. The signal-to-noise ratio was lower in the thermal oxidation spectra compared to the Oxone/KBr oxidation because of poor solubility in the deuterated solvent, presumably as a result of thermal crosslinking concurrent with the oxidation reaction. The growth of several small peaks (Figs. 11 and 12) may also indicate increased structural complexity as the polymers began to crosslink. The rate and exact temperature of these thermal oxidation reactions and how they can be decoupled from crosslinking will be further explored in a subsequent publication.

3.11. FTIR of the thermally oxidized TMBPF-DCDPS polymer

Fig. 13 shows the FTIR spectrum of the thermally oxidized TMBPF-DCDPS compared to the untreated sample. The thermally oxidized sample had significantly larger carbonyl peaks than the Oxone/KBr oxidized product in Fig. 7. This comparison of the FTIR

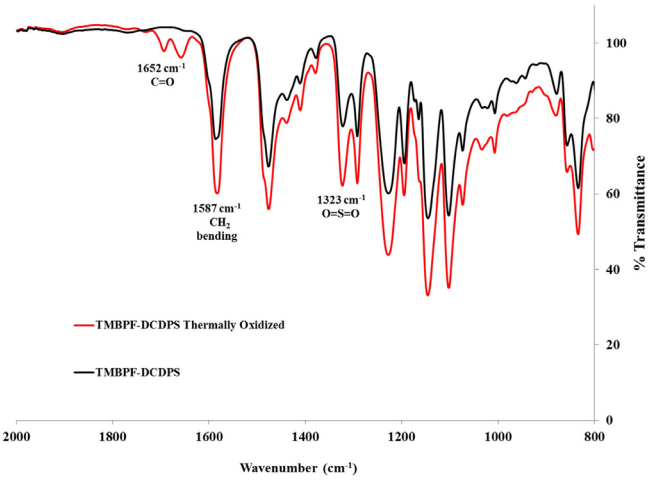

Fig. 13. IR of thermally oxidized TMBPF-DCDPS.

Table 2
Initial pure gas permeability of linear and crosslinked TMBPF-DFB.

	Gas permeability (Barrer) at 10 atm & 35 °C				
	O_2	N_2	CO_2	CH_4	H_2
TMBPF-DFB linear	2.8	0.52	10	0.54	29
TMBPF-DFB crosslinked	1.8	0.29	7.1	0.25	23
Bisphenol A polysulfone[a]	1.4	0.25	5.6	0.25	14
Tetramethyl bisphenol A polysulfone[a]	5.6	1.06	21	0.95	32

[a] Polysulfones [16]: CO_2, CH_4 at 10 bar and 35 °C; O_2, N_2, H_2 at 1 bar and 35 °C.

spectra supports the ^{1}H NMR result that thermal oxidation proceeds to higher conversion than Oxone/KBr conversion.

3.12. Initial gas transport results

As the effect of UV crosslinking on gas permeation properties was of interest for this research, gas transport results were obtained to compare the linear TMBPF containing poly(arylene ether ketone) and its UV crosslinked analog. A control film was cast from the TMBPF-DFB polymer and then cut in half. Permeabilities and selectivities of five different gases were directly tested on one half. The other half was exposed to UV irradiation to induce photochemical crosslinking. The mechanism for this photochemical reaction is benzylic hydrogen abstraction by an excited state benzophenone moiety [43,46], which has been shown to produce polyimides with high selectivity [19]. The gel fraction of this UV irradiated half was measured to be 100%, indicating that a highly crosslinked network was obtained. The density of the linear TMBPF-DFB polymer was 1.116 ± 0.003 g mL^{-1} and the density of the crosslinked TMBPF-DFB polymer was 1.146 ± 0.004 g mL^{-1}. The densification of the polymer membrane upon UV crosslinking was expected based on prior literature, and reflects a decrease in interchain spacing [47]. The pure gas permeabilities and selectivities of these two films are shown in Tables 2 and 3, where they are compared with bisphenol A polysulfone (UDEL) and a tetramethyl bisphenol A based polysulfone. The TMBPF-DFB linear polymer was un-oxidized and non-crosslinked, whereas the TMBPF-DFB crosslinked polymer was un-oxidized and crosslinked to afford a 100% gel fraction. The transport properties of the TMBPF-DFB linear and TMBPF-DFB crosslinked polymers are also shown in Fig. 14, where they are graphed with a commercial polysulfone, polyimide (Matrimid), and the 1991 and 2008 upper bounds.

The films demonstrate the expected relationship of crosslinking decreasing gas permeability and improving selectivity. An additional benefit of crosslinking for thin films is a reduction in physical aging [46]. The reduction of permeability after UV crosslinking has also been attributed to membrane densification [48]. Notably, the crosslinked TMBPF-DFB films had both higher permeability and selectivity compared to UDEL polysulfone. One reason for the greatly enhanced gas permeability of the TMBPF systems is the presence of the numerous bulky methyl groups along the polymeric backbone. These two samples represent a minor set that was obtainable from these TMBPF polymer series. In a subsequent publication, the effect of oxidation before and after UV crosslinking will be explored for both the TMBPF-DFB and the TMBPF-DCDPS polymers. The pure gas permeability was measured at five different pressures, which is graphed in Figs. 15 and 16.

Table 3
Initial pure gas selectivity of linear and crosslinked TMBPF-DFB.

	Gas selectivity at 10 atm & 35 °C				
	O_2/N_2	CO_2/CH_4	H_2/N_2	H_2/CH_4	CO_2/N_2
TMBPF-DFB linear	5.4	19	75	72	19
TMBPF-DFB crosslinked	6.2	28	79	92	24
Bisphenol A polysulfone[a]	5.6	22.4	56	56	22.4
Tetramethyl bisphenol A polysulfone[a]	5.3	22	30	34	19.8

[a] Polysulfones [16]: CO_2, CH_4 at 10 bar and 35 °C; O_2, N_2, H_2 at 1 bar and 35 °C.

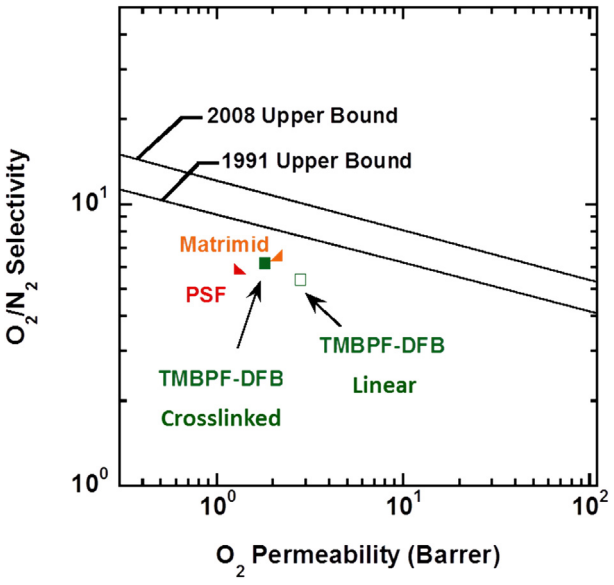

Fig. 14. Upper bound plot comparison of linear and crosslinked TMBPF-DFB [9].

4. Conclusions

In this paper, an economical route was presented to synthesize the TMBPF monomer and two TMBPF containing poly(arylene

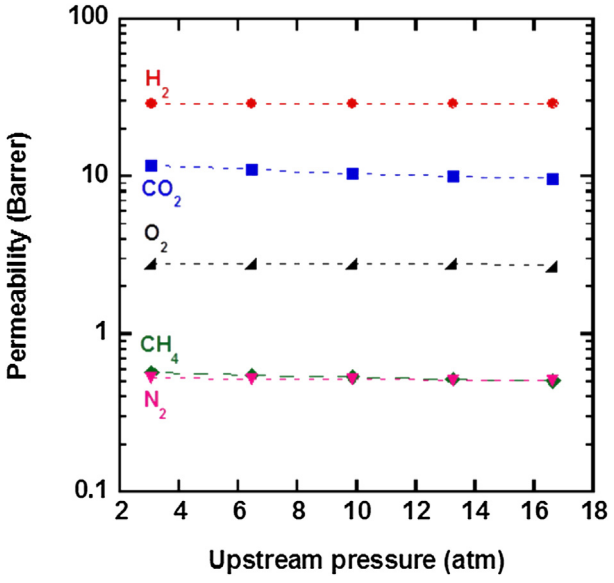

Fig. 15. Permeability as a function of feed pressure for linear TMBPF-DFB.

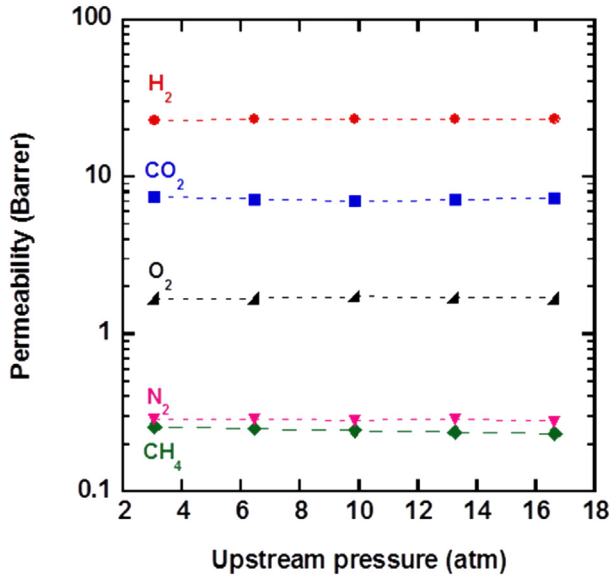

Fig. 16. Permeability as a function of feed pressure for crosslinked TMBPF-DFB.

ether) materials. High molecular weights were demonstrated quantitatively by SEC, and ductile films were obtained. The polymers are capable of backbone modifications that include oxidation and photochemical crosslinking. Solid state thermal oxidation of the benzylic methylene groups was more successful than solution oxidation, in terms of conversion. Both polymers were capable of producing crosslinked films with high gel fractions. ^{1}H NMR and FTIR spectroscopy were used for structural verification of the TMBPF monomer, TMBPF containing polymers, and conversion of the polymers to their oxidized form. The thermal oxidation reaction was also studied by TGA, and quantitative proof of the oxidation was presented by demonstrating theoretical weight gains. Initial gas transport properties demonstrated that crosslinking these polymers produced more highly selective membranes at the cost of reduced gas permeability.

Acknowledgments

The authors gratefully acknowledge the financial support of Air Products, Inc. (212-153-P), and the National Science Foundation under contracts (NSF-AIR: IIP-1237857) and (NSF-MRI: DMR-1126534).

References

[1] Bernardo P, Drioli E, Golemme G. Membrane gas separation: a review/state of the art. Ind Eng Chem Res 2009;48:4638.
[2] Baker RW, Lokhandwala K. Natural gas processing with membranes: an overview. Ind Eng Chem Res 2008;47:2109.
[3] Koros WJ, Fleming GK. Membrane-based gas separation. J Membr Sci 1993;83:1.
[4] Baker RW. Future directions of membrane gas separation technology. Ind Eng Chem Res 2002;41:1393.
[5] Robeson LM. Correlation of separation factor versus permeability for polymeric membranes. J Membr Sci 1991;62:165.
[6] Freeman BD. Basis of permeability/selectivity tradeoff relations in polymeric gas separation membranes. Macromolecules 1999;32:375.
[7] Doolittle AK. Newtonian flow. II. The dependence of the viscosity of liquids on free space. J Appl Phys 1951;22:1471.
[8] Cohen MH, Turnbull D. Molecular transport in liquids and glasses. J Chem Phys 1959;31:1164.
[9] Robeson LM. The upper bound revisited. J Membr Sci 2008;320:390.
[10] Min KE, Paul DR. Effect of tacticity on permeation properties of poly(methyl methacrylate). J Polym Sci Part B: Polym Phys 1988;26:1021.
[11] Miyata S, Sato S, Nagai K, Nakagawa T, Kudo K. Relationship between gas transport properties and fractional free volume determined from dielectric constant in polyimide films containing the hexafluoroisopropylidene group. J Appl Polym Sci 2008;107:3933.
[12] Stern SA. Polymers for gas separations: the next decade. J Membr Sci 1994;94:1.
[13] McHattie JS, Koros WJ, Paul DR. Gas transport properties of polysulfones. 1. Role of symmetry of methyl group placement on bisphenol. Polymer 1991;32:840.
[14] Kim I-W, Lee KJ, Jho JY, Park HC, Won J, Kang YS, et al. Correlation between structure and gas transport properties of silyl-modified polysulfones and poly(phenyl sulfone)s. Macromolecules 2001;34:2908.
[15] McHattie JS, Koros WJ, Paul DR. Gas transport properties of polysulfones. 2. Effect of bisphenol connector groups. Polymer 1991;32:2618.
[16] Aitken CL, Koros WJ, Paul DR. Effect of structural symmetry on gas transport properties of polysulfones. Macromolecules 1992;25:3424.
[17] Xiao Y, Chung T-S, Chng ML, Tamai S, Yamaguchi A. Structure and properties relationships for aromatic polyimides and their derived carbon membranes: experimental and simulation approaches. J Phys Chem B 2005;109:18741.
[18] Park HB, Jung CH, Lee YM, Hill AJ, Pas SJ, Mudie ST, et al. Polymers with cavities tuned for fast selective transport of small molecules and ions. Science 2007;318:254.
[19] Hayes RA. Polyimide gas-separation membranes. US4717393A, 1988.
[20] Bennett CL, Richards RE. Copolyimides for use as gas separation membranes. GB2244997A, 1991.
[21] Kita H, Inada T, Tanaka K, Okamoto K. Effect of photocrosslinking on permeability and permselectivity of gases through benzophenone-containing polyimide. J Membr Sci 1994;87:139.
[22] Ouyang M, Muisener RJ, Boulares A, Koberstein JT. UV-ozone induced growth of a SiOx surface layer on a cross-linked polysiloxane film: characterization and gas separation properties. J Membr Sci 2000;177:177.
[23] Kwisnek L, Heinz S, Wiggins JS, Nazarenko S. Multifunctional thiols as additives in UV-cured PEG-diacrylate membranes for CO2 separation. J Membr Sci 2011;369:429.
[24] Wind JD, Paul DR, Koros WJ. Natural gas permeation in polyimide membranes. J Membr Sci 2004;228:227.
[25] Shao L, Samseth J, Hagg M-B. Crosslinking and stabilization of high fractional free volume polymers for gas separation. Int J Greenh Gas Control 2008;2:492.
[26] Staudt-Bickel C, Koros WJ. Improvement of CO2/CH4 separation characteristics of polyimides by chemical crosslinking. J Membr Sci 1999;155:145.
[27] Lin H, Van Wagner E, Freeman BD, Toy LG, Gupta RP. Plasticization-enhanced hydrogen purification using polymeric membranes. Science 2006;311:639.
[28] Han G, Chung T-S, Toriida M, Tamai S. Thin-film composite forward osmosis membranes with novel hydrophilic supports for desalination. J Membr Sci 2012;423–424:543.
[29] Sun H, Zhang G, Liu Z, Zhang N, Zhang L, Ma W, et al. Self-crosslinked alkaline electrolyte membranes based on quaternary ammonium poly (ether sulfone) for high-performance alkaline fuel cells. Int J Hydrogen Energy 2012;37:9873.
[30] Macromolecular synthesis, vol. 1. New York: John Wiley & Sons; 1977.
[31] Hedrick JL, Mohanty DK, Johnson BC, Viswanathan R, Hinkley JA, McGrath JE. Radiation resistant amorphous-all aromatic polyarylene ether sulfones: synthesis, characterization, and mechanical properties. J Polym Sci Part A: Polym Chem 1986;24:287.
[32] Yin L, Wu J, Xiao J, Cao S. Oxidation of benzylic methylenes to ketones with Oxone–KBr in aqueous acetonitrile under transition metal free conditions. Tetrahedron Lett 2012;53:4418.
[33] Lin H, Freeman BD. In: Czichos H, S T, Smith L, editors. Spring handbook of metrology and testing. 2nd ed. Berlin: Springer; 2011. p. 426.
[34] Olah GA, Kobayashi S, Nishimura J. Aromatic substitution. XXXI. Friedel-Crafts sulfonylation of benzene and toluene with alkyl- and arylsulfonyl halides and anhydrides. J Am Chem Soc 1973;95:564.
[35] Bowman PJ, Brown BR, Chapman MA, Doyle PM. Synthesis and reactions of phenolic alkylbenzylnitrosamines. J Chem Res Synop 1984:72.
[36] Sanders DF, Smith ZP, Guo R, Robeson LM, McGrath JE, Paul DR, et al. Energy-efficient polymeric gas separation membranes for a sustainable future: a review. Polymer 2013;54:4729.
[37] Robeson LM, Farnham AG, McGrath JE. Synthesis and dynamic mechanical characteristics of poly(aryl ethers). Appl Polym Symp 1975;26:373.
[38] Rose JB. Preparation and properties of poly(arylene ether sulphones). Polymer 1974;15:456.
[39] Viswanathan R, Johnson BC, McGrath JE. Polymer 1984;25:1827.
[40] Bunnett JF. Mechanism and reactivity in aromatic nucleophilic substitution reactions. Q Rev Chem Soc 1958;12:1.
[41] Mohanty DK, Sachdeva Y, Hedrick JL, Wolfe JF, McGrath JE. Synthesis and transformations of tetramethyl bisphenol A polyaryl ethers. Polym Prepr (Am Chem Soc Div Polym Chem) 1984;25:19.
[42] Chen MS, White MC. Combined effects on selectivity in Fe-catalyzed methylene oxidation. Science 2010;327:566.
[43] Wright CT, Paul DR. Gas sorption and transport in UV-irradiated polyarylate copolymers based on tetramethylbisphenol-A and dihydroxybenzophenone. J Membr Sci 1997;124:161.

[44] Merkel TC, Zhou M, Baker RW. Carbon dioxide capture with membranes at an IGCC power plant. J Membr Sci 2012;389:441.
[45] Aitken CL, McHattie JS, Paul DR. Dynamic mechanical behavior of polysulfones. Macromolecules 1992;25:2910.
[46] McCaig MS, Paul DR. Effect of UV crosslinking and physical aging on the gas permeability of thin glassy polyarylate films. Polymer 1999;40:7209.
[47] Matsui S, Ishiguro T, Higuchi A, Nakagawa T. Effect of ultraviolet light irradiation on gas permeability in polyimide membranes. 1. Irradiation with low pressure mercury lamp on photosensitive and non-photosensitive membranes. J Polym Sci Part B: Polym Phys 1997;35:2259.
[48] Matsui S, Sato H, Nakagawa T. Effects of low molecular weight photosensitizer and UV irradiation on gas permeability and selectivity of polyimide membrane. J Membr Sci 1998;141:31.
[49] Sanders DF, Smith ZP, Ribeiro Jr CP, Guo R, McGrath JE, Paul DR, et al. Gas permeability, diffusivity, and free volume of thermally rearranged polymers based on 3,3′-dihydroxy-4,4′-diamino-biphenyl (HAB) and 2,2′-bis-(3,4-dicarboxyphenyl) hexafluoropropane dianhydride (6FDA). J Membr Sci 2012;409–410:232.
[50] Koros WJ, Chan AH, Paul DR. Sorption and transport of various gases in polycarbonate. J Membr Sci 1977;2:165.